Dalton Transactions

Accepted Manuscript

ROYAL SOCIETY OF CHEMISTRY

www.rsc.org/dalton

$K_2Sn_2ZnSe_6$, $Na_2Ge_2ZnSe_6$, and $Na_2In_2GeSe_6$: A New Series of Quaternary Selenides with Intriguing Structural Diversity and Nonlinear Optical Properties

Molin Zhou,[†,‡,§] Chao Li,[†,‡,§] Xiaoshuang Li,[†,‡,§] Jiyong Yao[†,‡,*] and Yicheng Wu[†,‡]

Three new compounds (*i.e.*, $K_2Sn_2ZnSe_6$, $Na_2Ge_2ZnSe_6$, and $Na_2In_2GeSe_6$) with intriguing structural diversity and nonlinear optical properties were discovered for the first time. They crystallize in space groups *P*4/*ncc*, *I*4/*mcm* and *Cc*, respectively. In $K_2Sn_2ZnSe_6$ and $Na_2Ge_2ZnSe_6$, the [Sn(Ge)Se_4] tetrahedra and [$ZnSe_4$] tetrahedra are linked via edge-sharing to build up a 1D [Sn_2ZnSe_6] infinite chain separated by K^+(Na^+) cations along the c direction, while the structure of $Na_2In_2GeSe_6$ is an interesting three-dimensional framework composed of [$InSe_4$] and [$GeSe_4$] tetrahedra via corner-sharing with Na^+ cations in the cavities. The experimental optical band gaps of these compounds were determined as 1.71(2) eV, 2.36(4) eV and 2.47(2) eV, respectively, according to UV-vis-NIR diffuse reflectance spectroscopy. Interestingly, in addition to the large band gap (1.80 eV for $AgGaSe_2$, as a comparison), $Na_2In_2GeSe_6$ exhibits phase-matchable nonlinear optical (NLO) property with a

[†]*Center for Crystal Research and Development, Technical Institute of Physics and Chemistry, Chinese Academy of Sciences, Beijing 100190, P.R. China*

[‡]*Key Laboratory of Functional Crystals and Laser Technology, Technical Institute of Physics and Chemistry, Chinese Academy of Sciences, Beijing 100190, P.R. China*

[§]*University of Chinese Academy of Sciences, Beijing 100049, P.R. China*

†Electronic supplementary information (ESI) available: Crystallographic data in CIF format for $K_2Sn_2ZnSe_6$, $Na_2Ge_2ZnSe_6$, and $Na_2In_2GeSe_6$

powder second harmonic generation signal about 0.8 times that of $AgGaS_2$. Moreover, $Na_2In_2GeSe_6$ melts congruently at a rather low temperature of 671 □, which suggests bulk crystals can be easily obtained by the Bridgman−Stockbarger method. Our preliminary results indicate that $Na_2In_2GeSe_6$ has promising applications in IR nonlinear optics.

Introduction

The research on metal chalcogenides has been a very active area owing to their great structural diversity and many important physical properties.[1-3] Recently, extensive exploration has been carried out in search for new Mid-far IR NLO materials in metal chalcogenides because IR NLO materials have great civil and military applications and the current commercially available chalcopyrite-type IR NLO crystals (*e.g.*, $AgGaS_2$,[4] $AgGaSe_2$[5] and $ZnGeP_2$[6]) have severe drawbacks.[7] Many new compounds with attractive NLO properties such as large NLO responses and large band gaps (possibly high laser damage thresholds) have been synthesized. Examples include $BaGa_4S_7$,[8] $BaGa_4Se_7$,[9] $BaGa_2MSe_6$ (M = Si, Ge; Q = S, Se),[10] $Pb_4Ga_4GeQ_{12}$ (Q = S, Se),[11] $Ba_{23}Ga_8Sb_2S_{38}$,[12] $Cs_5BiP_4Se_{12}$,[13] Ln_4GaSbS_9 (Ln = Pr, Nd, Sm, Gd−Ho),[14] and Ba_2InYQ_5 (Q = Se, Te),[15,16] $LiGaS_2$,[17] $LiGaSe_2$,[18] $Li_2In_2MS_6$ (M = Si, Ge),[19] $SnGa_4Q_7$ (Q = S, Se),[20] $AAsQ_2$ (A = Li,Na; Q = S,Se),[21] $AZrPSe_6$ (A = K, Rb, Cs)[1] and $Na_4MgM_2Se_6$ (M = Si, Ge).[22] Generally speaking, a large macroscopic NLO response originates from the cooperative arrangement of the microscopic NLO building units, including the MX_4 tetrahedra (M = Ga, In, Si, Ge, Sn *etc.*; X = S, Se), the polyhedra centered by the second-order Jahn-Teller (SOJT) distorted d^0 (*e.g.*, Ta^{5+}, Zr^{4+}) or d^{10} (*e.g.*, Ag^+, Zn^{2+}, Cd^{2+}) metal cations, and some polar structural units centered by cations with stereochemically active lone pair electrons (*e.g.*, As^{3+}, Sb^{3+}, Pb^{2+}). Meanwhile, it is well-known that the shorter and stronger interactions caused by smaller cations (*e.g.*, Li^+, Na^+, Mg^{2+}, K^+, Ca^{2+}) can draw the NLO-active microscopic groups closer to each other forming a denser packing to produce larger

NLO effects.[23–25] Besides, numerous exploration have proven that the inclusion of an alkali metal will effectively enlarge the band gap, which can in turn increase the laser damage threshold.[17–19]

In this work, we intended to combine different microscopic NLO-active building units with alkali metal into one compound to obtain new IR nonlinear optical materials. We thoroughly investigated the A-M-M'-Q (A = Na, K; M, M' = Ga, In, Ge, Sn, Zr, Zn, Cd, Sb, Pb; Q = S, Se) quaternary system and successfully discovered three new compounds $K_2Sn_2ZnSe_6$, $Na_2Ge_2ZnSe_6$, and $Na_2In_2GeSe_6$. The above compounds crystallize in space groups *P*4/*ncc*, *I*4/*mcm* and *Cc*, respectively. Although the former two crystallize in centrosymmetric structures, $Na_2In_2GeSe_6$ adopts a noncentrosymmetric (NCS) structure type and shows good NLO property with a large band gap of 2.47(2) eV, good phase-matchability and a powder second harmonic generation (SHG) response about 0.8 times that of benchmark $AgGaS_2$ at a laser radiation of 2.09 μm. Moreover, $Na_2In_2GeSe_6$ exhibits congruent-melting behavior with low melting point (671 □), which is very important for growing bulk single crystals for the practical application. In addition, $K_2Sn_2ZnSe_6$ and $Na_2Ge_2ZnSe_6$ clearly illuminate the influence of alkali cations on the packing of anionic groups, resulting in the intriguing structural diversity. Here, we report the syntheses, crystal structures, thermal, linear and nonlinear optical properties of the title compounds.

Experimental Section

Syntheses

The following reagents were used as obtained: Na (Sinopharm Chemical Reagent Co., Ltd, 99%), K (Sinopharm Chemical Reagent Co., Ltd, 99.9%), In (Sinopharm Chemical Reagent Co., Ltd, 99.9%), Ge (Sinopharm Chemical Reagent Co., Ltd, 99.9%), Sn (Sinopharm Chemical Reagent Co., Ltd, 99.9%), Se (Sinopharm Chemical Reagent Co., Ltd, 99.999%) and ZnS (Aladdin Co., Ltd, 99.9%). The binary starting materials Na_2Se, K_2Se, In_2Se_3, $GeSe_2$, and $SnSe_2$ were prepared by the stoichiometric reaction of the elements at high temperatures in sealed silica tubes evacuated to 10^{-3} Pa.

Traditional solid state reaction technique can be applied to grow the single crystals of the title compounds. During the process, all reactants were mixed and loaded into fused-silica tubes under an Ar atmosphere in a glovebox, then flame-sealed under a high vacuum of 10^{-3} Pa. The tubes were then placed in a computer-controlled furnace and heated. Compared with Na_2Se–In_2Se_3–$GeSe_2$ system, the $K(Na)_2Se$–$Sn(Ge)Se_2$–ZnSe system has higher sintering and melting temperatures. Thus, these compounds were heated to and cooled to different temperatures in our approach to obtain the single crystals. Detailed heating profiles are discussed below.

$K_2Sn_2ZnSe_6$ and $Na_2Ge_2ZnSe_6$. The mixtures of binary materials (K_2Se (0.5 mmol), $SnSe_2$ (1.1 mmol) and ZnSe (0.5 mmol) for $K_2Sn_2ZnSe_6$; Na_2Se (0.5 mmol), $GeSe_2$ (1.1 mmol) and ZnSe (0.5 mmol) for $Na_2Ge_2ZnSe_6$) were heated to 1273 K within 15 h, left for 48 h, cooled to 623 K at a rate of 3 K/h, and finally cooled to room

temperature by switching off the furnaces. Many prism-shaped crystals were found in the tubes for both compounds. The crystals are stable in air.

$Na_2In_2GeSe_6$. The mixtures of Na_2Se (0.5 mmol), In_2Se_3 (0.5 mmol) and $GeSe_2$ (0.5 mmol) were heated to 1173 K within 15 h, left for 48 h, cooled to 573 K at a rate of 3 K/h, and finally cooled to room temperature by switching off the furnace. Many chip-shaped crystals were found in the tubes. The crystals are stable in air.

Polycrystalline sample of $Na_2In_2GeSe_6$ was synthesized by mixtures of the corresponding binary materials in the stoichiometric ratio. The mixtures were heated to 973 K in 15 h and kept at that temperature for 48 h, and finally the furnaces were turned off.

Powder X-ray diffraction (PXRD) pattern of the ground powder was performed at room temperature on a Bruker D8 Focus diffractometer with Cu Kα (λ = 1.5418 Å) radiation. The scanning step width of 0.05º and a fixed counting time 0.2 s/step were applied to record the patterns in the 2θ range of 10–70º. The measured XRD powder pattern was found to match the simulated pattern generated using the CIF of the refined structure. (Figure 1).

Structure Determination

Single-crystal X-ray diffraction experiment was performed on a Rigaku AFC10 diffractometer equipped with a graphite-monochromated Mo-K_α (λ = 0.71073 Å) radiation at 293 K. The collection of the intensity data and cell refinement was carried

out with Crystalclear software.[26] Face-indexed absorption corrections were performed numerically with the use of the program XPREP.[27]

The structure was solved with the direct methods SHELXTLS program and refined with the least-squares program SHELXL of the SHELXTL.PC suite of programs.[27] Relevant crystallographic information from the single-crystal structure refinements are given in Table 1 and selected metrical distances are given in Table 2–4. Further information may be found in Supplementary Material.

Diffuse Reflectance Spectra

A Cary 5000 UV-vis-NIR spectrophotometer with a diffuse reflectance accessory was used to measure the spectra of the title compounds and $BaSO_4$ as a reference in the range 300 nm (4.1 eV) to 2000 nm (0.62 eV). Appropriate amounts of single crystals of the title compounds were thoroughly ground for the measurements.

Thermal Analysis

The thermal property of $Na_2In_2GeSe_6$ was investigated by the differential scanning calorimetric (DSC) analysis using the Labsys^{TM} TG-DTA16 (SETARAM) thermal analyzer. Appropriate amounts of small $Na_2In_2GeSe_6$ single crystals were manually selected and thoroughly ground into powder, and were then placed in a silica tube (5 mm o.d. × 3 mm i.d.) and sealed under a high vacuum. The heating and the cooling rates were both 15 K min^{-1}.

SHG Measurement

The optical SHG response of $Na_2In_2GeSe_6$ was measured by means of the Kurtz–Perry method.[28] The fundamental light was the 2090 nm light generated with a Q-switched Ho: Tm: Cr: YAG laser. Enough $Na_2In_2GeSe_6$ polycrystalline sample was ground to powder with the particle size range from 50−300 μm for the measurement. Microcrystalline $AgGaS_2$ of particle size (105−150 μm) served as a reference.

Results and Discussion

Crystal Growth

Three new quaternary selenides (*i.e.*, $K_2Sn_2ZnSe_6$, $Na_2Ge_2ZnSe_6$ and $Na_2In_2GeSe_6$) have been obtained by spontaneous nucleation method for the first time. We also tried to synthesize their sulfide and telluride analogues. Unfortunately, the sulfide crystals were of poor quality in our synthesis and no telluride analogues were found. Thus, we only report the study on those three selenides here.

Structures

$K_2Sn_2ZnSe_6$ belongs to the $K_2Sn_2MnSe_6$[29] structure type in space group *P*4/*ncc*, while $Na_2Ge_2ZnSe_6$ adopts the $KInSnSe_4$[30] structure type in space group *I*4/*mcm*. The asymmetric unit of $K_2Sn_2ZnSe_6$ contains two crystallographically independent K atoms, one Sn atom, one Zn atom and two independent Se atoms, occupying Wyckoff sites 4*c,* 4*c,* 8*e,* 4*b,* 16*g* and 8*f*, respectively, while the asymmetric unit of $Na_2Ge_2ZnSe_6$ contains one crystallographically independent Na atom, one Ge atom, one Zn atom and two independent Se atoms occupying Wyckoff sites 8*f,* 8*g,* 4*b,* 8*h* and 16*l*, respectively. All sites are occupied with occupancy of 100% in both compounds.

The arrangements of the structural units are similar between those two compounds, which are illustrated in Figure 2(a) and Figure 3(a). Their packing characteristic can be described as follows: two [Sn(Ge)Se_4] tetrahedra are first connected to each other by sharing two Se2 atoms to form the [Sn(Ge)$_2Se_6$] block, which is further linked via edge-sharing two Se1 atoms with one [$ZnSe_4$] tetrahedron to build up a 1D [Sn(Ge)$_2$$ZnSe_6$] infinite chain along the c direction. The chains are separated from each other by K(Na)$^+$ cations residing in the cavities. Figure 2(b) and Figure 3(b) demonstrate the coordination environments of K^+ and Na^+ cations, respectively. As is shown, all K^+ and Na^+ cations are coordinated by eight Se atoms in a bicapped trigonal prismatic arrangements. Moreover, The K and Sn in $K_2Sn_2ZnSe_6$ are more electropositive and larger than Na and Ge in $Na_2Ge_2ZnSe_6$, respectively, leading to the more loose packing and larger commensurate spaces for holding K^+.

Selected interatomic distances for the two compounds are displayed in Tables 2–3. For example, The Sn–Se distances and Se–Sn–Se angles are in the range of 2.4986(8)–2.5672(7) Å and 102.137(21)–117.340(16)°, respectively, which are comparable to those of 2.565(10)–2.582(1) Å and 115.180(57)° in $KSnSe_2$.[31] The Ge–Se bonds range from 2.3318(9) Å to 2.3929(9) Å with the Se–Ge–Se angles in the range of 96.177(8)°–114.081(20)°, which are in good agreement with those of 2.255(6)–2.395(10) Å and 97.651(31)–116.572(40)° in $Na_2Ge_2Se_5$.[32] In $K_2Sn_2ZnSe_6$, the Zn atom is bound to four Se atoms to form a $ZnSe_4$ tetrahedron and all the Zn–Se bonds share the same length 2.5142(7) Å with Se–Zn–Se angles ranging from 101.263(21)–113.725(21)°, while in $Na_2Ge_2ZnSe_6$, the Zn–Se bond distances and

Se–Zn–Se angles are 2.4833(7) Å and 96.054(22)–116.569(23)°, respectively. Such values are consistent with those in In_2ZnSe_4[33] (2.447 Å and 111.599°). The calculated bond valence sums (BVS)[34] (*i.e.*, 1.273, 1.173, 3.956, 1.840, 1.972 and 2.155 for K1, K2, Sn, Zn, Se1 and Se2 in $K_2Sn_2ZnSe_6$, respectively; 0.962, 3.905, 2.001, 1.938 and 1.970 for Na, Ge, Zn, Se1 and Se2 in $Na_2Ge_2ZnSe_6$, respectively) are close to the expected value, and further proves the validity of the atoms assignments.

As for $Na_2In_2GeSe_6$, it belongs to the $Li_2In_2MQ_6$ (M = Si, Ge; Q = S, Se)[19] structure type and crystallizes in the noncentrosymmetric space group *Cc* of the monoclinic system with unit cell parameters of a = 12.707(3) Å, b = 8.1157(16) Å, c = 12.760(3) Å, β = 108.70(3)° and Z = 4. In the asymmetric unit, there are two crystallographically independent Na atoms, two independent In atoms, one Ge atom, and six Se atoms. All atoms are at general positions with 100% occupancy, and there is no detectable disorder in the structure.

Fig 4(b) demonstrates the coordination environments of Na cations, the 5-coordinated Na1 atoms and 4-coordinated Na2 atoms are in a trigonal biyramidal and tetrahedral arrangements, respectively. Selected bond distances are listed in Table 4, for instance, the Na–Se distances of 2.863(1)–3.168(3) Å are in good agreement of $NaInSe_2$ (3.010 Å).[35] The distances of In–Se range from 2.558(2) to 2.571(3) Å, a little shorter than those in $NaInSe_2$ (2.758 Å).[35] The Ge–Se bond lengths of 2.335(1)–2.361(3) Å are a little longer than those of 2.313(1)–2.336(3) Å in $Ag_2In_2GeSe_6$.[36] The calculated bond valence sums (BVS)[34] (1.158, 1.245, 3.180, 3.220, 4.295, 1.869, 1.974, 2.134, 2.177, 2.071 and 2.167 for Na1, Na2, In1, In2, Ge,

Se1, Se2, Se3, Se4, Se5 and Se6, respectively) are also close to the expected value.

The crystal structure of $Na_2In_2GeSe_6$ is illustrated in Figure 4(a), it is an interesting three-dimensional framework composed of corner-sharing [$InSe_4$] and [$GeSe_4$] tetrahedra with Na^+ cations residing in the cavities. As is shown, the basic building unit of $Na_2In_2GeSe_6$ can be determined as a [$In_4Ge_2Se_{16}$] block comprised of two smaller [In_2GeSe_9] blocks. Firstly, two [$InSe_4$] tetrahedra, namely, [$In1Se_4$] and [$In2Se_4$], and one [$GeSe_4$] tetrahedron, are linked to each other via sharing corner Se2, Se3 and Se6 atoms to form a [In_2GeSe_9] block, which is further bridged with another [In_2GeSe_9] block by sharing corner Se1 and Se4 atoms. Then, the [$In_4Ge_2Se_{16}$] blocks are connected to each other by sharing corner Se5 atoms to generate the three-dimensional framework. Obviously that the alignment of [$GeSe_4$] groups is fully co-parallel while [$InSe_4$] tetrahedra deviate from the fully co-parallel alignment to some degree, the interplay of [$InSe_4$] and [$GeSe_4$] tetrahedra in this particular arrangements may increase the NLO properties.

Compared with the related $Li_2In_2GeSe_6$ compound, the larger and more ionic alkali metal Na^+ in $Na_2In_2GeSe_6$ acts as a counter ion to balance the negative charge of the $[In_2GeSe_6]^{2-}$ framework, while the smaller and more covalent Li^+ in $Li_2In_2GeSe_6$ becomes part of the complicated three-dimensional framework built by [$LiSe_4$], [$InSe_4$] and [$GeSe_4$] tetrahedra. It is obvious that different ionic radius and electronegativity of alkali metal cations have strong influences on the structures and properties of the materials.

Experimental Band Gaps

Figure 5 shows the UV-vis-NIR diffuse reflectance spectra of the title compounds in the region of 300-2000 nm. The experimental optical band gaps of 1.71(2) eV, 2.36(4) eV and 2.47(2) eV for $K_2Sn_2ZnSe_6$, $Na_2Ge_2ZnSe_6$, and $Na_2In_2GeSe_6$ respectively were determined by the straightforward extrapolation method.[37] Consequently the absorption edges are 725 nm, 525 nm and 502 nm, respectively. The band gaps are consistent with their colors. For the NLO compound $Na_2In_2GeSe_6$, the value is comparable to the common commercial crystals (*e.g.*, $AgGaS_2$–2.64 eV). Hence, $Na_2In_2GeSe_6$ may effectively avoid the two-photon absorption problem of the conventional 1(Nd:YAG) or 1.55(Yb:YAG) lasers, which has severely limited the application of the NLO $AgGaSe_2$ and $ZnGeP_2$ crystals.

Thermal Analysis

The DSC curve of $Na_2In_2GeSe_6$ is shown in Figure 6. It is clearly shown that $Na_2In_2GeSe_6$ melts congruently at a rather low temperature 671 □. This valuable thermal behavior makes it feasible to use the Bridgman–Stockbarger technique to grow bulk crystals, which are needed for the practical application. Additionally, the low melting point can effectively reduce the corrosion of the quartz tubes, which is helpful for single crystal growth with better quality. As a comparison, the melting points of several infrared crystals are much higher: (860 □ for $AgGaSe_2$, 915 □ for $LiGaSe_2$, 998 □ for $AgGaS_2$, 1025 □ for $ZnGeP_2$).

SHG Measurement

Owing to its non-centrosymmetric structure (NCS) structure, $Na_2In_2GeSe_6$ is expected to possess NLO properties. As shown in Figure 7, the SHG signal intensity of $Na_2In_2GeSe_6$ with the 2090 nm laser as the fundamental wavelength is about 0.8 times that of $AgGaS_2$ with a similar particle size 105–150 μm. Considering the large NLO effect of $AgGaS_2$, the above value is relatively large. In addition, the plot of SHG response versus particle size reveals the phase matching feature of $Na_2In_2GeSe_6$, which is an essential criteria for practical application. As the particle size increasing, the orientations of different particles change from canceling out each other to working in concert, until the saturation is reached. As discussed in the structure section that the alignment of $[GeSe_4]$ groups is fully co-parallel while $[InSe_4]$ tetrahedra deviate from the fully co-parallel alignment to some degree, such packing characteristics of the $[InSe_4]$ and $[GeSe_4]$ tetrahedra may explain the relatively large SHG response.

Conclusion

Single crystals of $K_2Sn_2ZnSe_6$, $Na_2Ge_2ZnSe_6$, and $Na_2In_2GeSe_6$ were grown and characterized for the first time. They possess the same stoichiometric ratio but crystallize in different space groups *P*4/*ncc*, *I*4/*mcm* and *Cc*, respectively due to the modification of metal cations with different electronegativities and ionic radii. The structures of $K_2Sn_2ZnSe_6$ and $Na_2Ge_2ZnSe_6$ are similar and can be described as $[Sn(Ge)Se_4]$ tetrahedra and $[ZnSe_4]$ tetrahedra are linked via edge-sharing to build up a 1D $[Sn_2ZnSe_6]$ infinite chain separated by $K^+(Na^+)$ cations along the c direction, while the structure of $Na_2In_2GeSe_6$ is an interesting three-dimensional framework

composed of [$InSe_4$] and [$GeSe_4$] tetrahedra via corner-sharing with Na^+ cations in the cavities. The experimental band gaps of these compounds were determined as 1.71(2) eV, 2.36(4) eV and 2.47(2) eV, respectively, according to UV-vis-NIR diffuse reflectance spectroscopy. Interestingly, in addition to the large band gap, $Na_2In_2GeSe_6$ exhibits a phase matchable feature NLO property with a powder SHG response at 2 μm that is approximately 0.8 times that of the benchmark material $AgGaS_2$ at a particle size of 105–150 μm. Moreover, $Na_2In_2GeSe_6$ melts congruently at a rather low temperature of 671 □, which makes it feasible to use the Bridgman–Stockbarger technique to grow bulk crystals needed for the practical application. Our preliminary experimental results suggest that $Na_2In_2GeSe_6$ has promising applications in IR nonlinear optics and further research is in progress.

Acknowledgments

This research was supported the National Natural Science Foundation of China (No. 51472251, and No. 21271178).

References

1. S. Banerjee, C. D. Malliakas, J. I. Jang, J. B. Ketterson and M. G. Kanatzidis, *J. Am. Chem. Soc.*, 2008, **130**, 12270.
2. T. K. Bera, J. I. Jang, J. B. Ketterson and M. G. Kanatzidis, *J. Am. Chem. Soc.*, 2009, **131**, 75.
3. W. Chen, G. Mouret, D. Boucher and F. K. Tittel, *Appl. Phys. B: Lasers Opt.*, 2001, **72**, 873.
4. G. D. Boyd, H. Kasper and J. H. Mcfee, *IEEE J. Quantum Electron.*, 1971, **7**, 563.
5. B. Tell and H. M. Kasper, *Phys. Rev. B: Solid State.*, 1971, **4**, 4455.
6. G. D. Boyd, E. Buehler and F. G. Storz, *Appl. Phys. Lett.*, 1971, **18**, 301.
7. P. G. Schunemann, *Aip Conf. Proc.*, 2007, **916**, 541.
8. X. S. Lin, G. Zhang and N. Ye, *Cryst. Growth Des.*, 2009, **9**, 1186.
9. J. Y. Yao, D. J. Mei, L. Bai, Z. S. Lin, W. L. Yin, P. Z. Fu and Y. C. Wu, *Inorg. Chem.*, 2010, **49**, 9212.
10. W. L. Yin, K. Feng, R. He, D. J. Mei, Z. S. Lin, J. Y. Yao and Y. C. Wu, *Dalton Trans.*, 2012, **41**, 5653.
11. Y. K. Chen, M. C. Chen, L. J. Zhou, L. Chen and L. M. Wu, *Inorg. Chem.*, 2013, **52**, 8334.
12. M. C. Chen, L. M. Wu, H. Lin, L. J. Zhou and L. Chen, *J. Am. Chem. Soc.*, 2012, **134**, 6058.
13. I. Chung, J. H. Song, J. I. Jang, A. J. Freeman, J. B. Ketterson and M. G.

Kanatzidis, *J. Am. Chem. Soc.*, 2009, **131**, 2647.

14. M. C. Chen, L. H. Li, Y. B. Chen and L. Chen, *J. Am. Chem. Soc.*, 2011, **133**, 4617.

15. W. L. Yin, K. Feng, W. D. Wang, Y. G. Shi, W. Y. Hao, J. Y. Yao and Y. C. Wu, *Inorg. Chem.*, 2012, **51**, 6860.

16. W. L. Yin, W. D. Wang, L. Bai, K. Feng, Y. G. Shi, W. Y. Hao, J. Y. Yao and Y. C. Wu, *Inorg. Chem.*, 2012, **51**, 11736.

17. Z. Z. Kish, V. V. Loshchak, E. Y. Peresh and E. E. Semrad, *Inorg. Mater.*, 1989, **25**, 1658.

18. V. Petrov, A. Yelisseyev, L. Isaenko, S. Lobanov, A. Titov and J. J. Zondy, *Appl Phys B-Lasers O*, 2004, **78**, 543.

19. W. L. Yin, K. Feng, W. Y. Hao, J. Y. Yao and Y. C. Wu, *Inorg. Chem.*, 2012, **51**, 5839.

20. Z. Z. Luo, C. S. Lin, H. H. Cui, W. L. Zhang, H. Zhang, Z. Z. He and W. D. Cheng, *Chem. Mater.*, 2014, **26**, 2743.

21. T. K. Bera, J. I. Jang, J. H. Song, C. D. Malliakas, A. J. Freeman, J. B. Ketterson and M. G. Kanatzidis, *J. Am. Chem. Soc.*, 2010, **132**, 3484.

22. K. Wu, Z. H. Yang and S. L. Pan, *Inorg. Chem.*, 2015, **54**, 10108.

23. H. W. Huang, J. Y. Yao, Z. Lin, X. Y. Wang, R. He, W. J. Yao, N. X. Zhai and C. T. Chen, *Chem. Mater.*, 2011, 23, 5457.

24. G. S. Yang, G. Peng, N. Ye, J. Y. Wang, M. Luo, T. Yan and Y. Q. Zhou, *Chem. Mater.*, 2015, **27**, 7520.

25. H. Huang, J. Yao, Z. Lin, X. Wang, R. He, W. Yao, N. Zhai and C. Chen, *Angew. Chem. Int. Edit.*, 2011, **50**, 10274.

26. Rigaku Corporation, Tokyo, Japan, CrystalClear 2008.

27. Sheldrick, G. M. *Acta. Crystallogr.*, *Sect. A: Fundam. Crystallogr.*, **2008**, *64*, 112.

28. Kurtz, S. K.; Perry, T. T. *J. Appl. Phys.*, **1968**, *39*, 3798.

29. X. Chen, X. Y. Huang, A. H. Fu, J. Li, L. D. Zhang and H. Y. Guo, *Chem. Mater.*, 2000, **12**, 2385.

30. S. J. Hwang, R. G. Iyer, P. N. Trikalitis, A. G. Ogden and M. G. Kanatzidis, *Inorg. Chem.*, 2004, **43**, 2237.

31. L. D. Zhang, Y. G. Wei, X. L. Feng and H. Y. Guo, *Chem J Chinese U*, 2005, **26**, 1395.

32. B. Eisenmann, J. Hansa and H. Schafer, *Rev Chim Miner*, 1984, **21**, 817.

33. L. Gastaldi, M. G. Simeone and S. Viticoli, *J. Solid State Chem.*, 1987, **66**, 251.

34. I. D. Brown and D. Altermatt, *Acta. Crystallogr., Sect. B*, 1985, **41**, 244.

35. R. Hoppe, W. Lidecke and F. C. Frorath, *Z. Anorg. Allg. Chem.*, 1961, **309**, 49.

36. O. V. Krykhovets, L. V. Sysa, I. D. Olekseyuk and T. Glowyak, *J. Alloys Compd.*, 1999, **287**, 181.

37. O. Schevciw and W. B. White, *Mater. Res. Bull.*, 1983, **18**, 1059.

Figure captions

Figure 1 Experimental (black) and simulated (red) X–ray powder diffraction data of $Na_2In_2GeSe_6$. The differences in peak intensity between the two patterns may be caused by the preferential orientation of the powder samples.

Figure 2 Crystal packing structure of $K_2Sn_2ZnSe_6$ with the unit cell marked, in which the red and turquoise polyhedra represent GeS_4 and ZnS_4 tetrahedra, respectively (a), coordination environments of K cations (b).

Figure 3 Crystal structure of the unit cell of $Na_2Ge_2ZnSe_6$, in which the red and turquoise polyhedra represent GeS_4 and ZnS_4 tetrahedra, respectively (a), coordination environments of Na cations (b).

Figure 4 Crystal packing characteristics of $Na_2In_2GeSe_6$ along the *b* axis with a single $[In_4Ge_2Se_{16}]$ group marked by a black circle, in which the red and turquoise polyhedra represent InS_4 and GeS_4 tetrahedra, respectively (a), coordination environments of Na cations (b).

Figure 5 Diffuse reflectance spectra of the title compounds.

Figure 6 DSC curve of $Na_2In_2GeSe_6$.

Figure 7 Oscilloscope traces of SHG signals for $Na_2In_2GeSe_6$ with $AgGaS_2$ as a reference at a particle size of 105–150 μm (a), Phase-matching curve for $Na_2In_2GeSe_6$ (*i.e.*, SHG response versus particle size) (b).

Figure 1

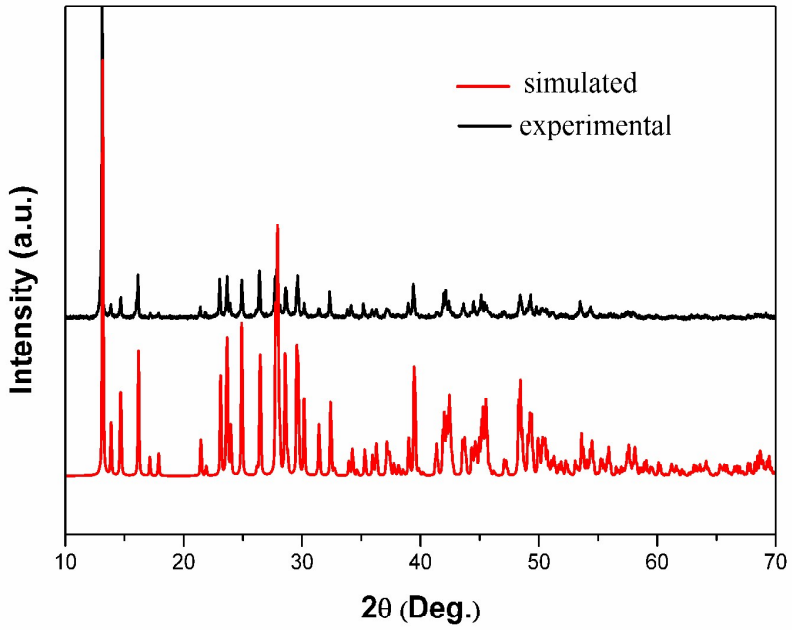

Figure 2

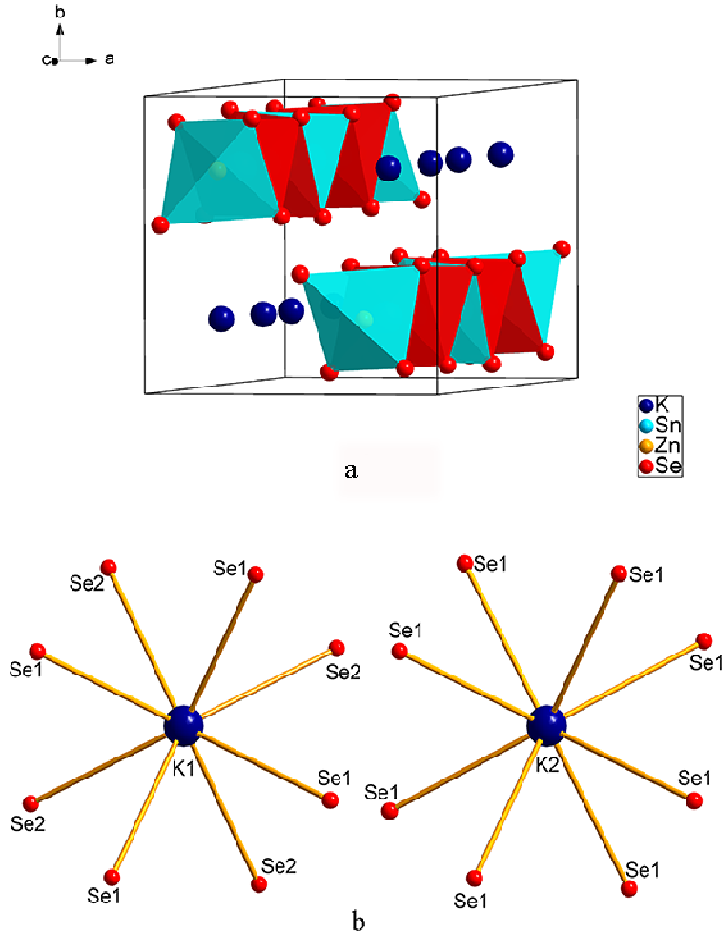

Figure 3

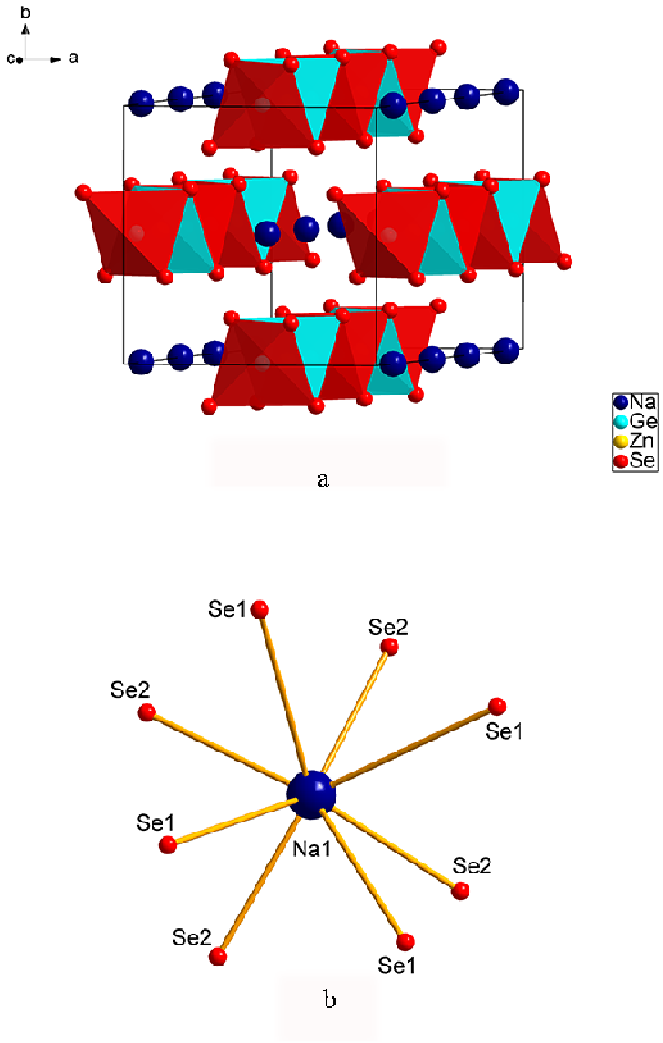

Figure 4

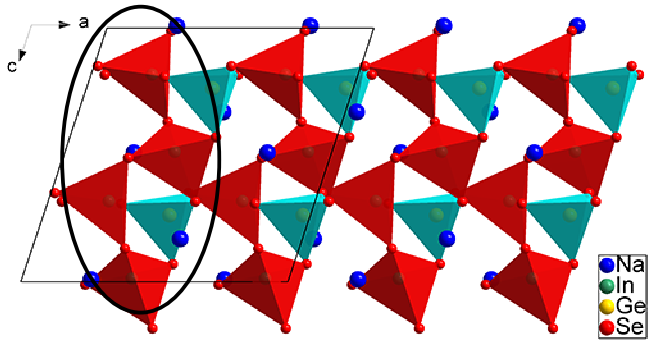

a

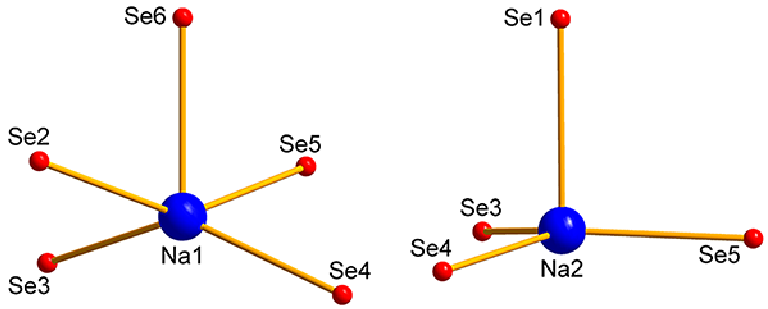

b

Figure 5

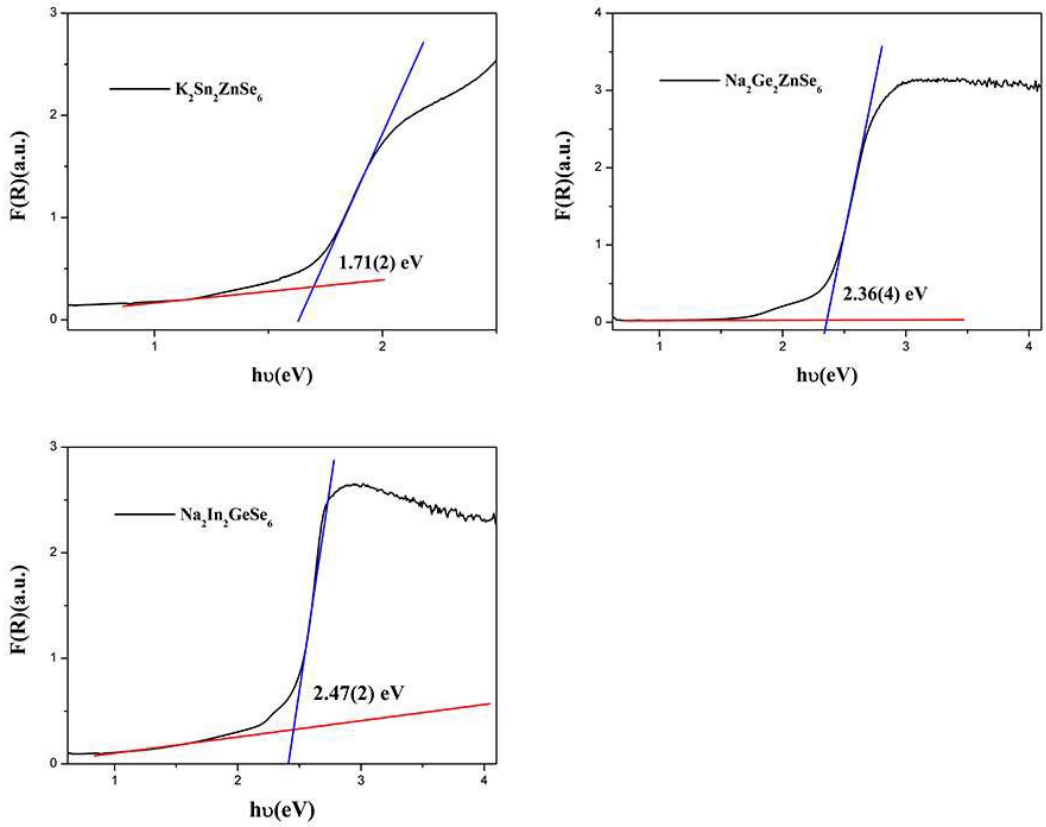

Figure 6

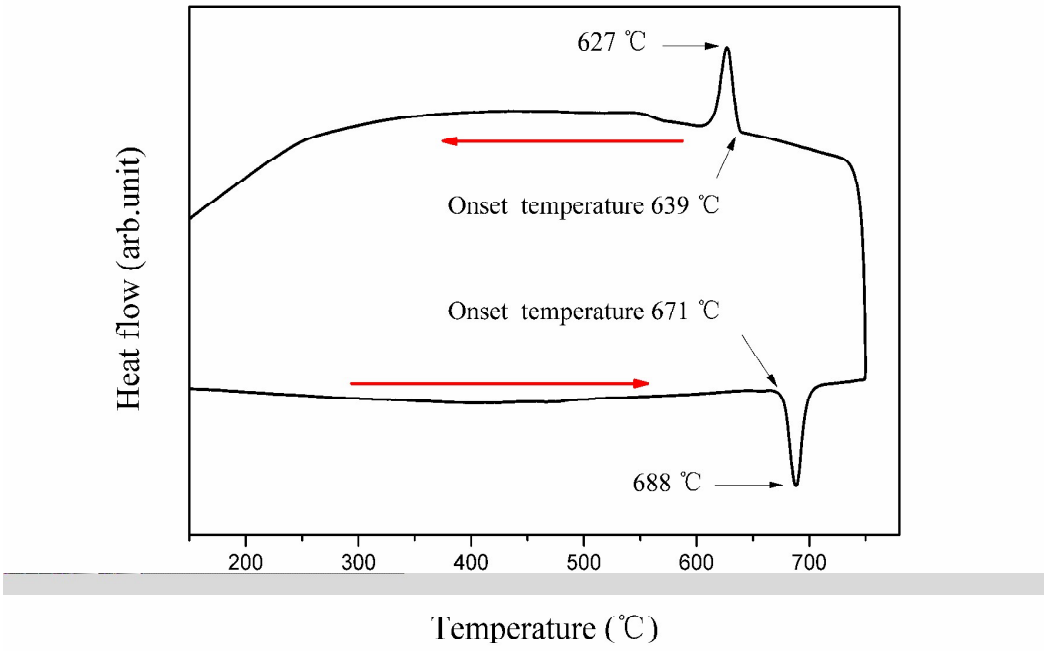

Figure 7

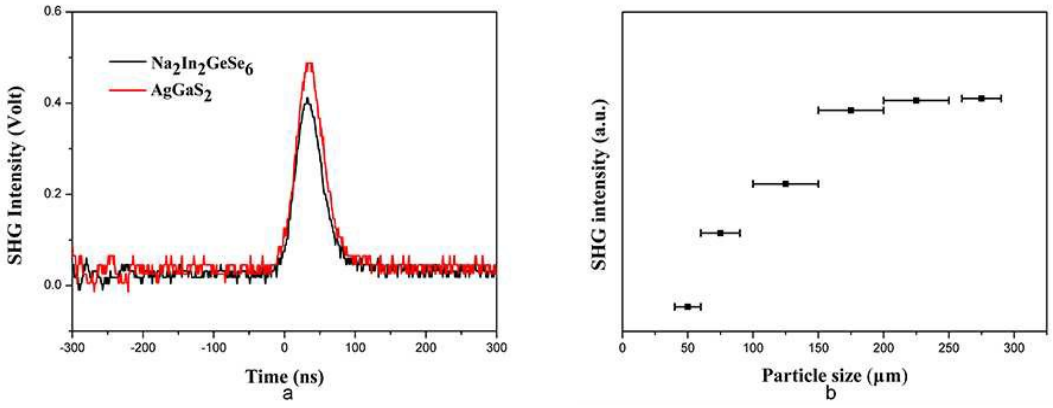

Table 1. Crystal data and structure refinement for $K_2Sn_2ZnSe_6$, $Na_2Ge_2ZnSe_6$, and $Na_2In_2GeSe_6$.

Chemial content	$K_2Sn_2ZnSe_6$	$Na_2Ge_2ZnSe_6$	$Na_2In_2GeSe_6$
Fw	854.71	730.29	821.97
a(Å)	8.1511(12)	7.7568(12)	12.707(3)
b(Å)	8.1511(12)	7.7568(12)	8.1157(16)
c(Å)	19.570(4)	18.734(4)	12.760(3)
β(°)	90	90	108.70(3)
Space group	*P*4/*ncc*	*I*4/*mcm*	*Cc*
V(Å^3)	1300.2(4)	1127.2(3)	1246.4(4)
Z	4	4	4
T(K)	293(2)	293(2)	293(2)
λ(Å)	0.71073	0.71073	0.71073
ρ_c(g/cm^3)	4.366	4.303	4.380
μ(mm^{-1})	23.024	26.797	23.597
R(F) [a]	0.0451	0.0451	0.0280
$R_W(F_o^2)$ [b]	0.0767	0.0998	0.0488

[a] $R(F) = \Sigma \| |F_o| - |F_c| | / \Sigma |F_o|$ for $F_o^2 > 2\sigma(F_o^2)$. [b] $R_W(F_o^2) = \{\Sigma [w(F_o^2 - F_c^2)^2] / \Sigma w F_o^4\}^{1/2}$ for all data. $w^{-1} = \sigma^2(F_o^2) + (zP)^2$, where $P = (\mathrm{Max}(F_o^2, 0) + 2F_c^2)/3$.

Table 2. Selected bond lengths(Å) for $K_2Sn_2ZnSe_6$.

K1–Se1	3.4589(18)×4	Sn–Se1	2.4986(8)×2
K1–Se2	3.3666(15)×4	Sn–Se2	2.5672(7)×2
K2–Se1	3.3359(13)×4	Zn–Se1	2.5142(7)×4
K2–Se1	3.5863(21)×4		

Table 3. Selected bond lengths(Å) for $Na_2Ge_2ZnSe_6$.

Na–Se1	3.6412(46)×4	Ge–Se2	2.3318(9)×2
Na–Se2	3.0019(22)×4	Zn–Se2	2.4833(7)×4
Ge–Se1	2.3929(9)×2		

Table 4. Selected bond lengths(Å) for $Na_2In_2GeSe_6$.

Na1–Se2	2.968(5)	In1–Se3	2.579(2)
Na1–Se3	2.876(5)	In1–Se4	2.568(3)
Na1–Se4	2.863(2)	In2–Se3	2.570(6)
Na1–Se5	3.234(2)	In2–Se4	2.557(7)
Na1–Se6	2.949(2)	In2–Se5	2.613(7)
Na2–Se1	3.168(5)	In2–Se6	2.599(2)
Na2–Se3	2.852(1)	Ge–Se1	2.335(1)
Na2–Se4	2.875(1)	Ge–Se2	2.341(9)
Na2–Se5	2.870(3)	Ge–Se5	2.361(3)
In1–Se1	2.615(2)	Ge–Se6	2.345(6)
In1–Se2	2.599(3)		

Table of Contents Entry

New selenides $K_2Sn_2ZnSe_6$, $Na_2Ge_2ZnSe_6$, and $Na_2In_2GeSe_6$ exhibit diverse structures and $Na_2In_2GeSe_6$ possesses a moderate second harmonic generation response.